Journal of Computer Science and Artificial Intelligence
ISSN: 3078-8242 (Print), ISSN: 3078-2309 (Online) | Vol. 7, No. 3, 2026

Event-Triggered Control for Course Tracking of Underactuated Ships Considering Actuator Faults

Shengda Ding

School of Navigation, Shandong Jiaotong University, Shandong 264200 China

Abstract: Addressing the course-keeping control problem of underactuated surface vessels subject to strong unknown environmental disturbances and asymmetric actuator saturation, this paper proposes an event-triggered (ETC) adaptive control scheme. A Radial Basis Function (RBF) neural network is constructed to approximate external disturbances and model uncertainties. To handle the impact of non-smooth asymmetric saturation nonlinearities, a continuously differentiable model based on the Gaussian error function is employed. An ETC is introduced to significantly reduce the frequency of controller updates, and a trajectory tracker is designed utilizing the backstepping method. The stability of the closed-loop system is theoretically proven via Lyapunov stability analysis. The control algorithm is simulated within the MATLAB environment to evaluate tracking performance. Simulation results demonstrate that the controller achieves precise and stable tracking, with the number of updates reduced by 1,056—amounting to a 44.0% reduction in communication resource utilization. This research provides a theoretical reference for the trajectory tracking of underactuated vessels under event-triggered mechanisms and asymmetric actuator constraints, with potential for further application in practical engineering.

Keywords: Event-Triggered Control, Adaptive Control, Neural Network, Input Saturation.

1. Introduction

Ship motion control, a core issue in the field of marine engineering, holds significant application value in scenarios such as autonomous navigation, dynamic positioning, and path tracking. The inherent nonlinear and strongly coupled characteristics of ship dynamics, combined with time-varying environmental disturbances such as wind, waves, and currents encountered during navigation, make it difficult for traditional control methods to achieve high-precision robust control [1]. Lin et al. [2] proposed a predictive PID controller based on PSO to achieve efficient and fast course-keeping for ships. Liang et al. [3] adopted a PID controller with time-varying gains to enhance the system's dynamic response, enabling it to withstand various wave conditions. Butt et al. [4] proposed integral sliding mode and integral super-twisting sliding mode controllers for ship course-keeping. To address issues such as slow error convergence, unknown ship speeds, and external environmental disturbances in ship trajectory tracking control, Liu et al. [5] proposed an observer-assisted global fast terminal sliding mode controller.

Although the aforementioned continuous control strategies have achieved significant results, traditional continuous sampling and updating mechanisms constantly occupy the communication links between sensors, controllers, and actuators. In large-scale ship or multi-ship cooperative scenarios, this not only easily causes communication congestion but also leads to frequent movements of ship steering gears with large inertia, resulting in mechanical wear and energy waste. Therefore, ETC, an on-demand allocation mechanism that updates the control law only when preset conditions are met, has been widely proposed and applied in complex system control [6-7], providing a new perspective for the efficient utilization of communication resources.

On the other hand, in practical marine engineering, controller design must account for the physical constraints of actuators. Affected by mechanical wear or hydraulic failures, steering gears often exhibit asymmetric saturation characteristics where the left and right limits are inconsistent. Ren et al. [8] discussed the design of ship course controllers under input saturation constraints; however, when combined with the backstepping method, the non-differentiable nature of traditional hard saturation models often leads to singularity problems. Meanwhile, the traditional backstepping method suffers from an inherent "explosion of complexity" defect. To address this, Liu et al. [9] introduced Dynamic Surface Control (DSC) technology to suppress the differential explosion, but the nonlinear uncertainties caused by high-order differential terms and complex environmental disturbances remain difficult to eliminate completely.

To tackle these uncertainty and nonlinear challenges, neural networks, relying on their powerful approximation capabilities, have become a mainstream tool for handling unknown model dynamics and disturbance compensation [10]. Shu et al. [11] successfully established a prediction model for ship energy consumption using BP neural networks; Deng et al. [12] further utilized RBF neural networks to effectively compensate online for ship model uncertainties and strong external disturbances.

In recent years, combining ETC with advanced algorithms for ship control has become a research hotspot. Liu et al. [13] and Deng et al. [14] introduced event-triggered mechanisms into ship path following and optimal trajectory tracking control, respectively, significantly reducing the update frequency. Gao et al. [15] and Ding et al. [16] further integrated Model Predictive Control (MPC) to propose event-triggered energy management and trajectory tracking strategies for hybrid ships. However, most existing studies have failed to effectively combine event-triggered mechanisms with asymmetric saturation faults, lacking a high-precision robust control scheme capable of both significantly reducing communication loads and smoothly handling the asymmetric constraints of actuators.

In summary, aiming at the course-keeping problem of underactuated ships subjected to strong unknown external disturbances and asymmetric saturated actuator faults, this

paper proposes a control method that integrates RBF neural network adaptive compensation and an asymmetric saturation event-triggered mechanism. The main contributions are as follows:

An RBF neural network is designed to approximate external disturbances and uncertain terms of the ship model, achieving the online estimation of composite uncertainties.

A continuously differentiable asymmetric saturation model based on the Gaussian error function is adopted to constrain the system, resolving the singularity problem caused by the non-differentiable nature of traditional hard saturation models.

An event-triggered mechanism is proposed to reduce the operating frequency of the actuator and decrease mechanical wear while ensuring system stability.

The global uniform ultimate boundedness of the closed-loop system is proven via Lyapunov theory, and the Zeno phenomenon is theoretically excluded.

2. Problem Analysis

2.1. Mathematical Model of the Ship Course Control System

To address the course-keeping problem of underactuated surface vessels, this paper adopts the classical second-order Nomoto model to describe the ship's steering dynamics. The state-space equations for the ship course system, as formulated by Kensaku Nomoto, are given as follows [17]:

$$\ddot{\phi}+\frac{1}{T}H\left(\dot{\phi}\right)=\frac{K}{T}\delta \tag{1}$$

Where δ is the rudder angle, ϕ is the heading angle, K is the turning index, and T is the follow-up index. $H\left(\dot{\phi}\right)$ is a nonlinear function of $\dot{\phi}$, which can be approximately expressed as:

$$H\left(\dot{\phi}\right)=a_1\dot{\phi}+a_2\dot{\phi}^3+a_3\dot{\phi}^5+\cdots \tag{2}$$

Where a_i , $i=1,2,3\cdots i$ are real-valued constants.

External marine environmental factors such as wind, waves, and currents exert significant disturbances on ship navigation. Additionally, ships exhibit obvious nonlinear hydrodynamic characteristics during maneuvering operations like steering and speed variation, rendering the heading control problem highly complex and uncertain. In actual navigation, besides sea-state disturbances, internal factors including propeller pulsation and hull mechanical vibration also introduce uncertain interference. Such disturbances are typically stochastic and time-varying, making precise modeling difficult. Based on Equations (1) and (2), a comprehensive disturbance term is introduced to uniformly characterize the aforementioned internal and external uncertainties, and finally a mathematical model of the ship's nonlinear heading control system that more closely aligns with real navigation conditions is established, with the specific form as follows:

$$\begin{cases}\dot{x}_1=x_2\\ \dot{x}_2=f(x_2)+bu+d(t)\\ y=x_1\end{cases} \tag{3}$$

Where $x_1=\phi$, $x_2=\dot{\phi}$, represent the ship's heading, heading rate, and input rudder angle, respectively. $f\left(x_1\right)$ is an unknown nonlinear function, $b=\frac{K}{T}$ is the control gain, y is the system output (heading), and $d(t)$ is the unknown external disturbance satisfying the above conditions.

Assumption 1: The unknown external environmental disturbance $d(t)$ and its time derivative are bounded, i.e., there exists an unknown positive constant $\left|d^*\right|$ such that $d(t)\le\left|d^*\right|$ holds.

Assumption 2: In the control system, the desired heading trajectory $y_d(t)$ is sufficiently smooth, and its first and second-order derivatives are known.

2.2. Modeling of Actuator Asymmetric Saturation Fault

Constrained by the physical limitations of the steering actuator itself, the ship's rudder angle input is typically subject to strict amplitude constraints. Once the control command exceeds the allowable range, it will not only degrade control accuracy but also potentially damage the system's dynamic performance and even cause instability. To address this, this paper designs and introduces an auxiliary compensation system to mitigate the adverse effects of rudder angle input saturation. This auxiliary system can monitor the steering actuator's operating status and control command amplitude in real time, and dynamically modify and compensate the control signal when the rudder angle enters the saturation region, thereby effectively alleviating the constraint of input saturation on control performance and improving the overall control effect and system robustness of the steering actuator under constrained conditions.

Considering the rudder angle input constraints with maximum value $u_{\max}$ and minimum value $-u_{\min}$, the maximum amplitude of the ship's rudder angle is $35°$.

$$-u_{\min}\le u\le u_{\max} \tag{4}$$

$$u=sat\left(v\right)=\begin{cases}u_{\max}, & v>u_{\max}\\ v, & -u_{\min}\le v\le u_{\max}\\ -u_{\min}, & v<-u_{\min}\end{cases} \tag{5}$$

Where v denotes the control input to be designed for the system.

Considering the effect of input saturation, the system is designed in the following form:

$$\dot{e}=\begin{cases}-c_{21}e-\frac{f\left(\cdot\right)}{e^2}e+\left(u-v\right), & |e|\ge\varepsilon\\ 0, & |e|<\varepsilon\end{cases} \tag{6}$$

Where e is the error term introduced by the auxiliary system to compensate for saturation, $c_{21}>0$ is a tunable parameter, and $z_2=x_2-a_2$ is the error variable. $f\left(\cdot\right)=f\left(z_2,\Delta u\right)=\left|z_2\cdot b\cdot\Delta u\right|+\frac{1}{2}\Delta u^2$, $\Delta u=u-v$

where ε is a designable positive parameter.

In practical marine engineering, actuators often exhibit asymmetric saturation constraints due to wear of the steering gear mechanical structure or faults in the hydraulic system, meaning the maximum limits for port and starboard rudder angles are inconsistent. To facilitate the subsequent backstepping design of the controller, this paper abandons the non-differentiable traditional hard saturation model and adopts a continuously differentiable model based on the Gaussian error function to smoothly approximate the asymmetric saturation characteristics:

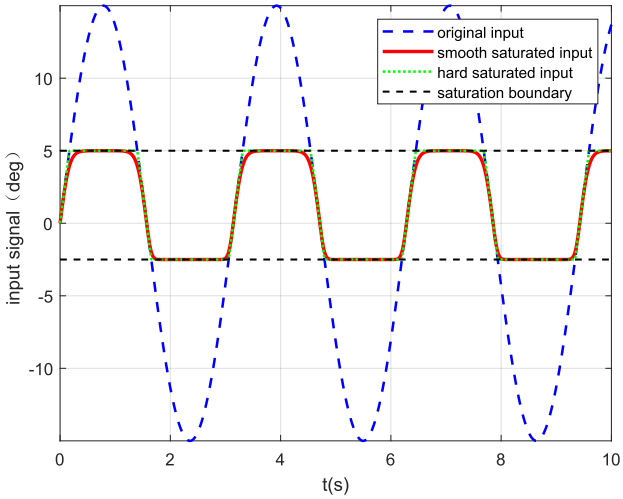

Figure 1. Comparison of Asymmetric Saturated Actuator Responses

$$\mathrm{sat}(u)=\tau_M\times\mathrm{erf}\left(\frac{\sqrt{\pi}}{2\tau_M}u\right) \tag{7}$$

Where $\tau_M=\frac{\tau^+ +\tau^-}{2}+\frac{\tau^+ -\tau^-}{2}\mathrm{sign}(u)$, τ^+ and τ^- denote the upper and lower bounds of the actuator, $\mathrm{sign}(\cdot)$ is the standard sign function, and $\mathrm{erf}(\cdot)$ is the Gaussian error function, defined as $\mathrm{erf}(x)=\frac{2}{\sqrt{\pi}}\int_0^x \mathrm{e}^{-t^2}\mathrm{d}t$. Figure 1 shows that Equation (7) can indeed guarantee the implementation of saturation constraints in a smooth form, where $\tau^+=5$, $\tau^-=-2.5$, and the input signal is $\varphi(t)=15\sin(2t)$.

2.3. Design of RBF Neural Network

Since $f(x_1)$ and the external disturbance $d(t)$ contain strong nonlinearities and uncertainties, this paper introduces an RBF neural network for online approximation and compensation. In this paper, the RBF is used to approximate continuous functions.

$$\begin{aligned} h_{nn}(Z)&=\theta^{\mathrm{T}}\xi(Z)\\ h(Z)&:R^q\to R \end{aligned} \tag{8}$$

Where $Z\in\Omega_Z\subset R^q$ is the input vector, $\theta=[\theta_1,\theta_2,\ldots\theta_l]^{\mathrm{T}}\in R^l$ is the weight vector, and $\xi(Z)=[\xi_1(Z),\xi_2(Z),\ldots,\xi_l(Z)]^{\mathrm{T}}$ is the radial basis function vector. In this paper, the Gaussian function is chosen as the radial basis function of the hidden layer:

$$\xi_i(Z)=\exp\left[\frac{-(Z-\mu_i)^{\mathrm{T}}(Z-\mu_i)}{\eta_i^2}\right],i=1,2,\ldots,l \tag{9}$$

Where $\mu_i=[\mu_{i1},\mu_{i2}\ldots,\mu_{iq}]^{\mathrm{T}}$ is the center position vector of the Gaussian function, and η_i is its width.

$$h(Z)=\theta^{*\mathrm{T}}\xi(Z)+\delta^*,\forall Z\in\Omega_Z \tag{10}$$

Where θ^* is the ideal constant weight, and δ^* is the approximation error. For all $Z\in\Omega_Z$, when $\delta_m>0$, there exists an ideal constant weight θ^* such that $|\delta^*|\le\delta_m$. The physical meaning of the ideal weight θ^* is the optimal value that minimizes the global approximation error, which is specifically defined as:

$$\theta^*\overset{\Delta}{=}\arg\min_{\theta\in R^l}\left\{\sup_{Z\in\Omega_Z}\left|h(Z)-\theta^T\xi(Z)\right|\right\} \tag{11}$$

2.4. Design of ETC

Traditional ship heading control usually relies on the Time-Triggered Control mechanism, where the controller performs sampling and control signal transmission at a fixed period. However, in the actual marine engineering environment, continuous high-frequency control commands not only occupy a large amount of the system's limited communication bandwidth but also cause frequent and slight movements of the ship's steering gear with large inertia. Such high-frequency movements are likely to cause severe wear of the mechanical structure and result in ineffective energy consumption. To address this, this paper introduces a dynamic ETC mechanism based on a hybrid threshold, aiming to allocate communication and control resources on demand—specifically, control update commands are only sent to the actuator when there is a significant deviation in the system state that truly requires correction. The trigger error of the control quantity is defined as:

$$e_u(t)=v(t)-u_k(t) \tag{12}$$

Where $v(t)$ is the ideal control input calculated at the current time, and $u_k(t)$ is the discrete hold signal that was actually transmitted to the ship's steering gear and is being executed at the last ETC.

The ETC is designed as:

$$t_{k+1}=\inf\{t>t_k|\ \ \|e_u(t)\|\ge\mu\|Z(t)\|+m\} \tag{13}$$

where $\mu\in(0,1)$ is the relative threshold coefficient, and $m>0$ is the absolute trigger dead-zone parameter. When the trigger error violates the above boundary, the system records the current time as t_{k+1} and updates the actuator input; otherwise, the actuator maintains the previous state using a zero-order holder.

3. Controller Design

Step 1: Define Error Variables

$$z_1 = x_1 - y_d \tag{14}$$

Taking the time derivative of z_1 yields:

$$\dot{z}_1 = x_2 - \dot{y}_d \tag{15}$$

To limit the abrupt jump of the virtual control signal when the initial error is large, this paper introduces a smooth bounded nonlinear reshaping function $\rho_1(z_1) = \tanh(z_1 / \lambda_1)$, which is combined with the RBF neural network to preliminarily approximate the kinematic unmodeled dynamics. The virtual control law is chosen as:

$$\alpha_2 = -c_1\rho_1(z_1) - \hat{\theta}_1^{\mathrm{T}}\xi_1(Z) + \dot{y}_d \tag{16}$$

Where $c_1 > 0, \lambda_1 > 0$ are tunable parameters, and $\hat{\theta}$ is the estimate of θ.

To avoid repeated differentiation of α_2, a first-order low-pass filter is introduced, and the virtual control law is passed through this filter to obtain the filtered state variable β_2:

$$\tau_0\dot{\beta}_2 + \beta_2 = \alpha_2, \beta_2(0) = \alpha_2(0) \tag{17}$$

Where $\tau_0 > 0$ is the time constant of the filter. The filtering error can thus be defined as $\eta_2 = \beta_2 - \alpha_2$.

Substituting (16) into (15) yields:

$$\dot{z}_1 = -c_1 p(z_1) - \hat{\theta}_1^{\mathrm{T}}\xi_1(Z) + \dot{y}_d \tag{18}$$

Choose the Lyapunov function

$$V_1 = \frac{1}{2}z_1^{\,2} \tag{19}$$

Taking the time derivative yields:

$$\dot{V}_1 = z_1\dot{z}_1 \tag{20}$$

Substituting (19) into (21) yields:

$$\dot{V}_1 = -c_1\rho_1(z_1)\cdot z_1 + z_1 z_2 - z_1\hat{\theta}_1^{\mathrm{T}}\xi_1(Z) \tag{21}$$

Step 2: Define Error Variables

$$z_2 = x_2 - \beta_2 \tag{22}$$

Taking the time derivative of z_2 yields:

$$\dot{z}_2 = \dot{x}_2 - \dot{\beta}_2 = f(x_2) + bu + d(t) - \dot{\beta}_2 \tag{23}$$

Let the total dynamic uncertainty be $F_2(X) = f(x_2) + d(t)$, which is online approximated by the RBF neural network, i.e., $F_2(X) = \theta^{*\mathrm{T}}\xi(Z) + \delta^*$.

Considering the faults and physical constraints of the ship's steering actuator, there is an inevitable saturation deviation between the actual output rudder angle $u(t)$ and the command $v(t)$ issued by the controller, defined as $\Delta u = \tau(u) - v(t)$. To eliminate the destructive effect of this deviation on the closed-loop system stability, the following nonlinear anti-windup auxiliary compensation system $e(t)$ is designed:

$$\dot{e} = \begin{cases} -c_{21}e - \dfrac{|z_2\Delta u| + 0.5\Delta u^2}{e^2}e + \Delta u, & |e| \geq \varepsilon \\ 0, & |e| < \varepsilon \end{cases} \tag{24}$$

Where $c_{21} > 0$ is a tunable parameter, and ε is a designable positive parameter.

Combined with the backstepping method, the control law is designed as follows:

$$v = \frac{1}{b}\left[-c_1\rho_1(z_1) - c_2\rho_2(z_2) - \hat{\theta}_2^{\mathrm{T}}\xi_2(Z) + e + \dot{\beta}_2\right] \tag{25}$$

Where $c_2 > 0$, $\rho_2(z_2) = \tanh(z_2 / \lambda_2)$, and $\hat{\theta}$ is the estimate of θ^*, whose online update laws are given as:

$$\dot{\hat{\theta}}_1 = \Gamma_1[z_1\xi_1(Z) - \sigma_1\hat{\theta}_1] \tag{26}$$

$$\dot{\hat{\theta}}_2 = \Gamma_2[z_2\xi_2(Z) - \sigma_2\hat{\theta}_2] \tag{27}$$

Where Γ_1, Γ_2 are positive definite learning rate matrices, and $\dot{\hat{\theta}}$ is the time derivative of the estimate to avoid parameter drift. $\sigma_1, \sigma_2 > 0$ are robust leakage coefficients, which are used to prevent the weights from drifting under persistent external disturbances.

To significantly reduce the communication load of the controller and the actuation frequency of the steering gear, an absolute error triggering strategy is introduced, and the ETC is designed as:

$$t_{k+1} = \inf\{t > t_k \,|\, |z_1(t)| > \delta\} \tag{28}$$

Where $\delta > 0$ is the preset absolute event-triggered threshold. When the error violates this threshold, the trigger time is updated to t_{k+1}, and the system sends the latest command $u(t) = v(t_{k+1})$; otherwise, $u(t)$ remains unchanged as the previous command $v(t_k)$.

After the ship's steering actuator receives the command $u(t)$, constrained by the physical structure of the asymmetric fault, the actual generated rudder angle $\tau(u)$ follows a smooth asymmetric saturation response model composed of the Gaussian error function:

$$\tau(u) = \mathrm{sat}(u) = u_M \cdot \mathrm{erf}\left(\frac{\sqrt{\pi}}{2u_M}u\right) \tag{29}$$

Where the adaptive asymmetric dynamic center u_M depends on the sign polarity of the command:

$$u_M = \frac{u_{\max} + u_{\min}}{2} + \frac{u_{\max} - u_{\min}}{2}\text{sign}(u) \tag{30}$$

Through this continuously differentiable asymmetric model, the system not only avoids the singularity problem of traditional piecewise hard saturation at the inflection point, but also cooperates with the auxiliary system in Eq. (24) to achieve global stable tracking within the constrained domain of asymmetric faults.

4. Stability Analysis

4.1. Stability Proof

Choose the Lyapunov function

$$V_2 = V_1 + \frac{1}{2}z_2^2 + \frac{1}{2}\eta_2^2 + \frac{1}{2}e^2 + \frac{1}{2}\tilde{\theta}_i^{\mathrm{T}}\Gamma_i^{-1}\tilde{\theta}_i \tag{31}$$

Taking the time derivative of V yields:

$$\dot{V} = z_1\dot{z}_1 + z_2\dot{z}_2 + \eta_2\dot{\eta}_2 + e\dot{e} - \tilde{\theta}_i^{\mathrm{T}}\Gamma_i^{-1}\dot{\hat{\theta}}_i \tag{32}$$

Substituting $\dot{z}_1 = z_2 + \eta_2 + \alpha_2 - \dot{y}_d$ and combining with the virtual control law (16), we have:

$$z_1\dot{z}_1 = -c_1 z_1\rho_1(z_1) + z_1 z_2 + z_1\eta_2 + z_1\tilde{\theta}_1^{\mathrm{T}}\xi_1(Z) + z_1\delta_1^* \tag{33}$$

According to Young's inequality: $z_2\varepsilon_2 \le \frac{1}{2}z_2^2 + \frac{1}{2}\varepsilon_2^2$, $z_2 e \le \frac{1}{2}z_2^2 + \frac{1}{2}e^2$.

Substituting (23) yields

$$z_2\dot{z}_2 = -c_2 z_2\rho_2(z_2) - z_1 z_2 + z_2\tilde{\theta}_2^T\xi_2(Z) + z_2\delta^*{}_2 + z_2 e + bz_2\Delta u \tag{34}$$

According to Young's inequality: $z_2\varepsilon_2 \le \frac{1}{2}z_2^2 + \frac{1}{2}\delta^{*2}{}_2$,

$$\begin{aligned}\dot{V}_2 \le & -\left[c_1\frac{\rho_1(z_1)}{z_1} - 1\right]z_1^2 \\ & -\left[c_2\frac{\rho_2(z_2)}{z_2} - \frac{3}{2}\right]z_2^2 \\ & -\left(\frac{1}{\tau_0} - 1\right)y_1^2 - (k_e - 1)e^2 \\ & -\frac{\sigma_1}{2}\|\tilde{\theta}_1\|^2 - \frac{\sigma_2}{2}\|\tilde{\theta}_2\|^2 \\ & +\left(\frac{1}{2}\delta^{*2}{}_1 + \frac{1}{2}\delta^{*2}{}_2 + \frac{1}{2}M_1^2 + \frac{b^2+1}{2}\Delta u_{\max}^2 + \frac{\sigma_1}{2}\|\theta_1^*\|^2 + \frac{\sigma_2}{2}\|\theta_2^*\|^2\right)\end{aligned} \tag{40}$$

By choosing c_1, c_2, k_e and a sufficiently small filter constant τ_0, the following positive definite convergence parameter μ can be defined:

$$z_2 e \le \frac{1}{2}z_2^2 + \frac{1}{2}e^2.$$

Substituting the weight update laws (26) and (27) into (31), the following inequality can be obtained:

$$\sigma_i\tilde{\theta}_i^{\mathrm{T}}\hat{\theta}_i \le -\frac{\sigma_i}{2}\|\tilde{\theta}_i\|^2 + \frac{\sigma_i}{2}\|\theta_i^*\|^2, \quad (i = 1, 2) \tag{35}$$

For the anti-windup auxiliary system, its derivative term satisfies:

$$e\dot{e} \le -k_e e^2 - |z_2 b\Delta u| + e\Delta u \le -k_e e^2 + \frac{1}{2}e^2 + \frac{1}{2}\Delta u^2 \tag{36}$$

Taking the time derivative of the filtering error η_2 yields:

$$\dot{\eta}_2 = \dot{\beta}_2 - \dot{\alpha}_2 = -\frac{\eta_2}{\tau_0} - \dot{\alpha}_2 \tag{37}$$

Denote $\dot{\alpha}_2$ as the function $B_1(\cdot)$. Since all signals in the closed-loop system are bounded, we reasonably assume that this derivative has an unknown maximum upper bound M_1, i.e., $|B_1(\cdot)| \le M_1$.

$$\eta_2\dot{\eta}_2 = -\frac{\eta_2^2}{\tau_0} - \eta_2 B_1(\cdot) \tag{38}$$

According to Young's inequality: $|\eta_2 B_1(\cdot)| \le \frac{1}{2}\eta_2^2 + \frac{1}{2}B_1(\cdot)^2$.

Substituting $|B_1(\cdot)| \le M_1$ yields:

$$|\eta_2 B_1(\cdot)| \le \frac{1}{2}\eta_2^2 + \frac{1}{2}M_1^2 \tag{39}$$

Substituting all the above scaling inequalities back into Eq. (32), we obtain:

$$\mu = \min\left\{ \begin{array}{l} 2\left(c_1 \dfrac{\rho_1(z_1)}{z_1} - 1\right), 2\left(c_2 \dfrac{\rho_2(z_2)}{z_2} - \dfrac{3}{2}\right), 2\left(\dfrac{1}{\tau_0} - 1\right), \\ 2(k_e - 1), \dfrac{\sigma_1}{\lambda_{\max}(\Gamma_1^{-1})}, \dfrac{\sigma_2}{\lambda_{\max}(\Gamma_2^{-1})} \end{array} \right\} \tag{41}$$

Meanwhile, all pure constant terms are organized as:

$$\begin{aligned} C_0 &= \frac{1}{2}\delta_1^{*2} + \frac{1}{2}\delta_2^{*2} + \frac{1}{2}M_1^2 \\ &+ \frac{b^2+1}{2}\Delta u_{\max}^2 + \frac{\sigma_1}{2}\| \theta_1^*\|^2 + \frac{\sigma_2}{2}\| \theta_2^*\|^2 \end{aligned} \tag{42}$$

In summary, we obtain:

$$\dot{V}_2 \le -\mu V_2 + C_0 \tag{43}$$

According to the Lyapunov stability theorem, all signals in the closed-loop system are uniformly ultimately bounded.

4.2. Zeno Phenomenon Avoidance

In ETC, it is necessary to theoretically exclude the possibility of infinite triggers within finite time to ensure the physical feasibility of hardware actuators.

Assume that the times of two consecutive triggers are t_k and t_{k+1}, respectively. Within the trigger interval $\Delta t = t_{k+1} - t_k$, the derivative of the control command is defined as:

$$\frac{d}{dt}|z_1(t)| = \text{sign}(z_1(t)) \cdot \dot{v}(t) \le |\dot{v}(t)| \tag{44}$$

Since it has been rigorously proven in the previous section that all signals in the closed-loop system are bounded, there must exist a global positive constant $M_v > 0$ such that the derivative of the continuous control signal satisfies $|\dot{v}(t)| \le M_v$.

Integrating Eq. (44) over the interval $[t_k, t_{k+1}]$. At the trigger instant, $z_1 = 0$, and at the critical point of the next trigger, the system must violate the absolute trigger threshold. Thus, we obtain:

$$\delta = |z_1(t_{k+1})| - |z_1(t_k)| \le \int_{t_k}^{t_{k+1}} |\dot{v}(t)|\, dt \le M_v(t_{k+1} - t_k) \tag{45}$$

It can be solved that the minimum time interval between two consecutive trigger events satisfies:

$$t_{k+1} - t_k \ge \frac{\delta}{M_v} > 0 \tag{46}$$

Since the preset trigger parameter δ and the signal upper bound M_v are both constants strictly greater than 0, this implies that there must exist a minimum time interval absolutely greater than 0 between two consecutive event triggers. Therefore, the ETC proposed in this study not only effectively reduces the control update frequency but also completely avoids the Zeno phenomenon in theory, ensuring the engineering practicability of the control algorithm.

5. Simulation Verification

To verify the effectiveness and robustness of the proposed neural network adaptive heading control algorithm based on the event-triggered mechanism, a simulation platform for the underactuated ship heading closed-loop control system is built in the MATLAB environment in this section. The simulation is based on the research of the "Yulong" ship from Dalian Maritime University [18]. The "Yulong" ship has a length of 126.0 m, a beam of 20.8 m, a full-load draft of 8.0 m, a block coefficient of 0.681, and a speed of 7.7 m/s. The parameters of the ship's Nomoto model are calculated as $c_1 = 0.25$, $c_2 = 200$, $c_{21} = 0.5$, $\Gamma_1 = diag\{0.001\}$, $\Gamma_2 = diag\{0.01\}$, the time constant of the dynamic surface filter is $\tau_0 = 0.3$, the total simulation step size of the system is $T_s = 0.5s$, the total simulation duration is 1200 s, and the initial value of e is 20.

The simulation results are as follows:

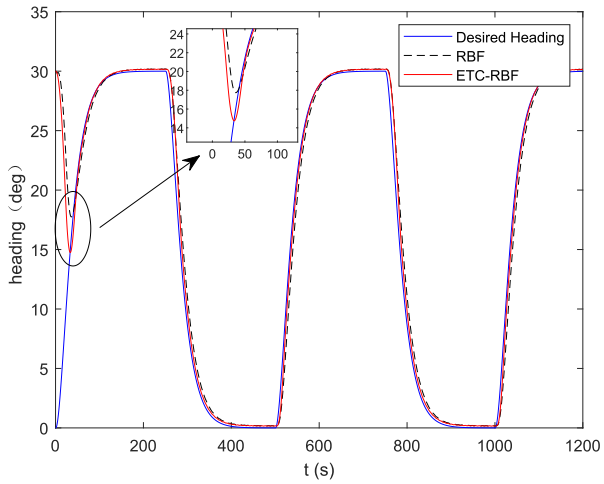

Figure 2. Time Response of Curve of Ship Course

Figure 2 shows the time-history response curves of the ship's heading under severe sea state disturbances. Observing the transient response phase, the proposed algorithm can drive the system to converge rapidly to the set heading within 40s when facing a large initial deviation of 30°, and can track the desired heading faster than the traditional RBF algorithm.

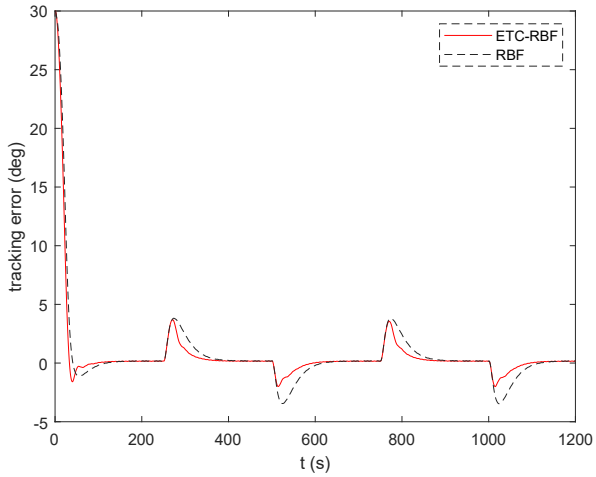

Figure 3. Time-history Curve of Ship Tracking Error

Figure 3 presents the ship's heading tracking error. From the overall trend, the heading tracking errors of both the ETC and the traditional neural network control can maintain a low level for most of the time, achieving effective tracking to a certain extent. The ETC-RBF algorithm proposed in this paper exhibits prominent advantages: at the initial moment, the heading tracking error converges rapidly to nearly 0 with a faster convergence speed; in the steady-state phase, the error fluctuation amplitude is smaller, resulting in more stable ship heading. The error peak value is lower than that of the traditional neural network control, and the algorithm has stronger ability to suppress error growth when responding to local disturbances, with higher tracking accuracy.

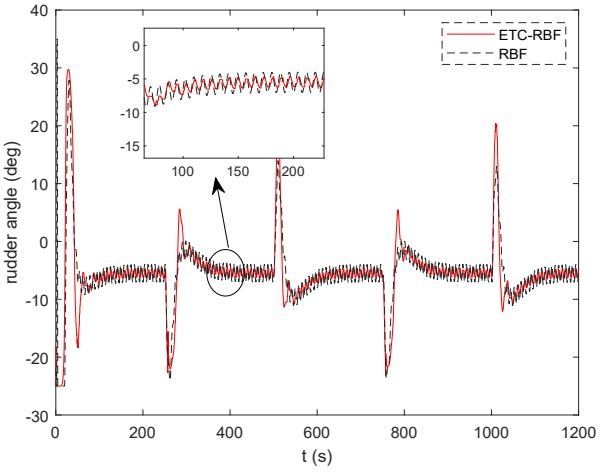

Figure 4. Time Response of Ship Rudder Angle

Figure 4 shows the time-history curve of the ship's input rudder angle. From the local details of Figure 4, it can be seen that the proposed algorithm not only strictly limits the rudder angle within the physically feasible range of [-25°, 35°], but also effectively suppresses the high-frequency oscillatory components of the control signal. The rudder angle output exhibits high smoothness, which greatly ensures the operational safety and service life of the steering gear system.

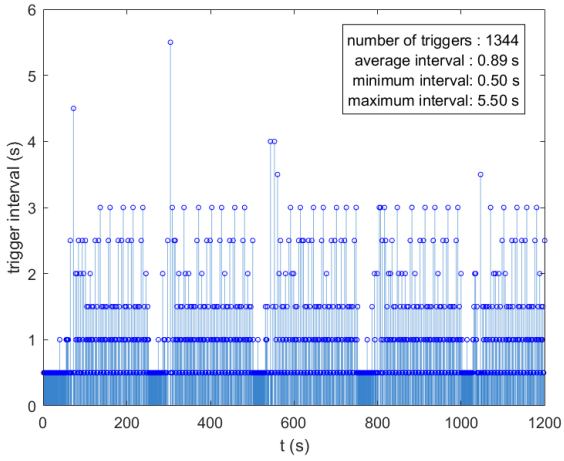

Figure 5. ETC Control Intervals

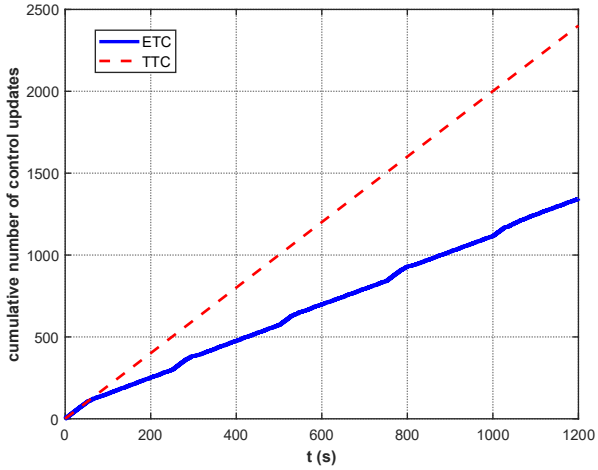

Figure 6. Cumulative Process of ETC Occurrences

Figure 5 (event-triggered interval distribution) and Figure 6 (cumulative event-trigger count step plot) intuitively demonstrate the core advantage of the proposed ETC mechanism in saving system communication resources. Within the 1200 s simulation period, the traditional time-triggered control (TTC) based continuous control method must operate at a fixed period (0.5s), occupying the communication link 2400 times in total; in contrast, the algorithm in this section, while maintaining extremely high tracking accuracy, drastically reduces the cumulative trigger update count to only 1344 times.

As shown in Figure 5, the system adaptively shortens the sampling interval when the heading deviation is large or disturbances change abruptly; when the system enters a steady state or the error falls within the dead-zone pipeline, the communication channel remains silent, and the actuator maintains the current rudder angle via a zero-order holder, with the maximum trigger interval dynamically extended to 5.5s. The proposed event-triggered strategy saves up to 44.0% of communication resources.

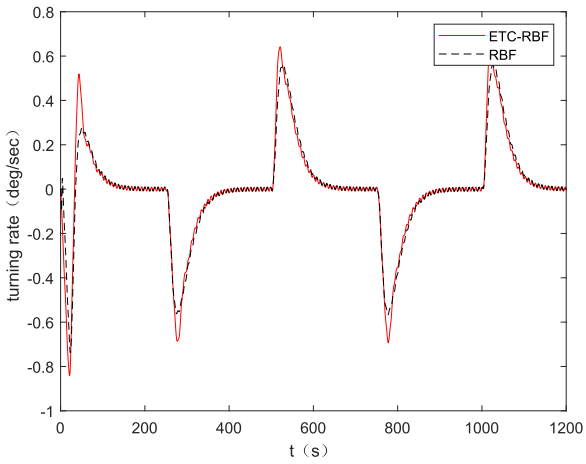

Figure 7. Time Response of Ship Yaw Rate

Figure 7 shows the time-history curve of the ship's yaw rate. Overall, the ship's yaw rate under both event-triggered control and traditional neural network control exhibits fluctuating changes. In the initial stage, the yaw rate of the proposed algorithm is faster, enabling the ship to quickly enter a stable sailing state with higher response efficiency.

6. Conclusion

This paper proposes an event-triggered adaptive control algorithm. Based on RBF neural networks, an ETC is designed, which ensures that the ETC interval is greater than 0 through the difference between the control signal and the trigger signal, effectively avoiding the Zeno phenomenon. The robustness, rapidity, and stability of the algorithm are proven through theoretical derivation. The simulation results show that the controller can maintain precise trajectory tracking, and the number of updates is reduced by 1056 times, cutting the ship's communication resource occupation by 44.0%, which verifies the effectiveness of the algorithm. In practice, it helps to reduce ship energy consumption and improve the maneuverability and safety of the ship.

References

[1] Zhang, Y., Zhang, J., & Sui, B. (2024). Robust fixed-time adaptive fault-tolerant control for dynamic positioning of ships with thruster faults. Applied Sciences, 14(13), 5738. https://doi.org/10.3390/app14135738

[2] Lin, B., Zheng, M., Han, B., et al. (2024). PSO-based predictive PID-backstepping controller design for the course-keeping of ships. Journal of Marine Science and Engineering, 12(2), 202. https://doi.org/10.3390/jmse12020202

[3] Liang, L., Cheng, Q., Li, J., et al. (2024). Roll reduction non-linear controller based on rudder and fin joint for ship. Ships and Offshore Structures, 19(11), 1900–1911. https://doi.org/10.1080/17445302.2024.2311642

[4] Butt, M. M., Butt, A. I. K., & Ahmad, I. (2025). Integral sliding mode and integral supertwisting sliding mode control for ship course-keeping. IEEE Access. https://doi.org/10.1109/ACCESS.2025.3498721

[5] Liu, W., Zhang, X., Zhang, H., et al. (2025). Observer-assisted global fast terminal sliding mode control of trajectory tracking for underactuated ship. Ocean Engineering, 325, 120721. https://doi.org/10.1016/j.oceaneng.2025.120721

[6] Han, J., Jiang, H., Zhao, Y., et al. (2025). Fixed-time event-triggered and periodic event-triggered containment control for heterogeneous multi-agent systems under DoS attacks. Systems & Control Letters, 204, 106208. https://doi.org/10.1016/j.sysconle.2025.106208

[7] de Souza, C., Tarbouriech, S., Queinnec, I., et al. (2024). Nonstandard anti-windup approach for event-triggered control purpose. Systems & Control Letters, 185, 105715. https://doi.org/10.1016/j.sysconle.2024.105715

[8] Ren, Y., Zhang, L., Ying, Y., et al. (2023). Model-parameter-free prescribed time trajectory tracking control for under-actuated unmanned surface vehicles with saturation constraints and external disturbances. Journal of Marine Science and Engineering, 11(9), 1717. https://doi.org/10.3390/jmse11091717

[9] Liu, S., Zhang, G., Zhang, W., et al. (2022). Robust fuzzy dynamic surface formation control for underactuated ships using MLP and LFG. Systems Science & Control Engineering, 10(1), 272–281. https://doi.org/10.1080/21642583.2022.2082624

[10] Guzelbulut, C., Badalotti, T., Fujita, Y., et al. (2024). Artificial neural network-based route optimization of a wind-assisted ship. Journal of Marine Science and Engineering, 12(9), 1645. https://doi.org/10.3390/jmse12091645

[11] Shu, Y., Yu, B., Liu, W., et al. (2024). Investigation of ship energy consumption based on neural network. Ocean & Coastal Management, 254, 107167. https://doi.org/10.1016/j.ocecoaman.2024.107167

[12] Deng, Z., Cui, J., Zhu, Z., et al. (2025). Adaptive trajectory tracking control of underactuated ships using parameter prediction based neural network. Ocean Engineering, 329, 121188. https://doi.org/10.1016/j.oceaneng.2025.121188

[13] Liu, C., Li, T., Wu, W., et al. (2024). Event-triggered predictive path following control of autonomous ships with an MMG model. Ocean Engineering, 314, 119582. https://doi.org/10.1016/j.oceaneng.2024.119582

[14] Deng, Y., Zhang, S., Xu, Y., et al. (2024). Event-triggered optimal trajectory tracking control of underactuated ships based on goal representation heuristic dynamic programming. Ocean Engineering, 308, 118251. https://doi.org/10.1016/j.oceaneng.2024.118251

[15] Gao, D., Chen, L., & Wang, Y. (2024). An energy trade-off management strategy for hybrid ships based on event-triggered model predictive control. International Journal of Electrical Power & Energy Systems, 162, 110312. https://doi.org/10.1016/j.ijepes.2024.110312

[16] Ding, Q., Deng, F., Du, Z., et al. (2024). FTUDE based event-triggered NMPC for trajectory tracking of dynamic positioning ships under input constraints. Ocean Engineering, 314, 119682. https://doi.org/10.1016/j.oceaneng.2024.119682

[17] Tong, S., Sui, S., & Li, Y. (2015). Observed-based adaptive fuzzy tracking control for switched nonlinear systems with dead-zone. IEEE Transactions on Cybernetics, 45(12), 2816–2826. https://doi.org/10.1109/TCYB.2014.2383791

[18] Li, T. S., Wang, D., Feng, G., et al. (2009). A DSC approach to robust adaptive NN tracking control for strict-feedback nonlinear systems. IEEE Transactions on Systems, Man, and Cybernetics, Part B (Cybernetics), 40(3), 915–927. https://doi.org/10.1109/TSMCB.2009.2032264